

1 Revision 1 – 06/02/2021

2
3 Zolenskyite, FeCr₂S₄, a new sulfide mineral from the Indarch meteorite

4 Chi Ma^{1,*} and Alan E. Rubin^{2,3}

5 ¹Division of Geological and Planetary Sciences, California Institute of Technology,
6 Pasadena, CA 91125, USA

7
8 ²Department of Earth, Planetary, and Space Sciences, University of California,
9 Los Angeles, CA 90095-1567, USA

10
11 ³Maine Mineral & Gem Museum, 99 Main Street, P.O. Box 500,
12 Bethel, ME 04217, USA

13
14
15 **ABSTRACT**

16 Zolenskyite (IMA 2020-070), FeCr₂S₄, is a new sulfide mineral that occurs within troilite, with
17 clinoenstatite and tridymite, in the matrix of the Indarch meteorite, an EH4 enstatite chondrite. The
18 mean chemical composition of zolenskyite determined by electron probe microanalysis, is (wt%)
19 S 43.85, Cr 35.53, Fe 18.94, Mn 0.68, Ca 0.13, total 99.13, yielding an empirical formula of
20 Fe_{0.99}Mn_{0.04}Ca_{0.01}Cr_{1.99}S_{3.98}. The ideal formula is FeCr₂S₄. Electron back-scatter diffraction shows
21 that zolenskyite has the *C2/m* CrNb₂Se₄-Cr₃S₄-type structure of synthetic FeCr₂S₄, which has *a* =
22 12.84(1) Å, *b* = 3.44(1) Å, *c* = 5.94(1) Å, β = 117(1)°, *V* = 234(6) Å³, and *Z* = 2. The calculated
23 density using the measured composition is 4.09 g/cm³. Zolenskyite is a monoclinic polymorph of
24 daubréelite. It may be a high-pressure phase, formed from daubréelite at high pressures (several
25 GPa) and moderate temperatures in highly shocked regions of the EH parent asteroid before
26 becoming incorporated into Indarch via impact mixing. Zolenskyite survived moderate annealing
27 of the Indarch whole-rock. The new mineral is named in honor of Michael E. Zolensky, an
28 esteemed cosmochemist and mineralogist at NASA's Johnson Space Center, for his contributions
29 to research on extraterrestrial materials, including enstatite chondrites.

30
31 **Keywords:** zolenskyite, FeCr₂S₄, new mineral, sulfide mineral, Indarch meteorite, enstatite
32 chondrite.

33
34 *E-mail: chima@caltech.edu

36

INTRODUCTION

37 The Indarch meteorite, which fell at Shusha, Azerbaijan on April 7, 1891, is an EH4
38 enstatite chondrite (Meteoritical Bulletin Database). The meteorite consists of (in wt%):
39 72.6% silicates (clinoenstatite and disordered orthoenstatite, averaging $\text{En}_{98.3}\text{Fs}_{1.1}\text{Wo}_{0.6}$;
40 albite, averaging $\text{Ab}_{97.6}\text{An}_{1.6}\text{Or}_{0.8}$; tridymite), 17.5% Si-bearing low-Ni metallic Fe (kamacite),
41 7.3% Ti-, Cr-, Mn- and Zn-bearing troilite, 1.0% niningerite, 0.39% oldhamite, trace amounts
42 of rudashevskyite (Fe,Zn)S, 0.05% FeCr_2S_4 (listed as daubréelite, but is actually mainly
43 zolenskyite, the new phase described here from the Indarch matrix, that in some cases is
44 intimately intergrown with cronusite and schöllhornite – terrestrial weathering products of
45 caswellsilverite and oldhamite), 1.1% schreibersite, 0.04% graphite, and trace amounts of
46 cohenite, lawrencite, and nierite Si_3N_4 (e.g., Mason 1966; Keil 1968). During a
47 nanomineralogical investigation of polished thick sections of Indarch, we identified the new
48 sulfide mineral, FeCr_2S_4 with the monoclinic $C2/m$ CrNb_2Se_4 - Cr_3S_4 -type structure, which we
49 named “zolenskyite” (Fig. 1). All the FeCr_2S_4 in the Indarch matrix that we found is
50 zolenskyite; one sulfide-rich patch containing daubréelite is present within a porphyritic
51 pyroxene chondrule (Fig. 2). To characterize the chemical composition and structure of
52 zolenskyite (as well as its associated phases), we used field-emission scanning electron
53 microscopy (SEM), electron back-scatter diffraction (EBSD), and electron probe
54 microanalysis (EPMA). Synthetic FeCr_2S_4 and $(\text{Fe}_{0.6}\text{Cr}_{0.4})\text{Cr}_2\text{S}_4$ with the $C2/m$ CrNb_2Se_4 -
55 Cr_3S_4 -type structure have been reported (Tressler et al. 1968; Lutz et al. 1983); presented here
56 is the first natural occurrence of this phase as a new mineral in a chondritic meteorite.

57 **MINERAL NAME AND TYPE MATERIAL**

58 The new mineral and its name have been approved by the Commission on New
59 Minerals, Nomenclature and Classification of the International Mineralogical Association
60 (IMA 2020-070) (Ma 2021). The mineral name is in honor of Michael E. Zolensky (born in
61 1955), esteemed planetary scientist, cosmochemist and mineralogist at NASA's Johnson
62 Space Center for his outstanding contributions to research on extraterrestrial materials,
63 including enstatite chondrites. Caltech sections ICM1, ICM2, ICM3 and ICM6, taken from
64 facing slices of the Indarch meteorite, contain the type material of zolenskyite. Section ICM3,
65 hereafter referred to as USNM 7926, has been deposited in the Smithsonian Institution's
66 National Museum of Natural History, Washington DC, USA, under catalogue USNM 7926.
67 USNM 7926 also contains rare grains of joegoldsteinite (MnCr_2S_4 ; Isa et al. 2016).

68 **OCCURRENCE AND APPEARANCE**

69 Zolenskyite occurs within troilite, associated with clinoenstatite and tridymite in the
70 Indarch matrix in sections ICM1, ICM6, and USNM 7926 (Fig. 1). Zolenskyite occurs as euhedral-
71 subhedral single crystals, $\sim 10 - 20 \mu\text{m}$ in size, with oxidation alteration patches within each grain.
72 Only the brighter clean regions (up to $2 \mu\text{m}$ in size) in the backscattered electron images are the
73 type material of zolenskyite, whereas the darker regions are oxidized areas (Fig. 1).
74 Zolenskyite is opaque. Color, luster, streak, hardness, tenacity, cleavage, fracture, density, and
75 optical properties could not be determined because of the small grain size, but are likely close to
76 those of its Cr-analog brezinaite (Cr_3S_4). All occurrences of FeCr_2S_4 in the Indarch matrix are
77 zolenskyite. The only occurrence of daubr elite we encountered in Indarch is associated with
78 troilite and is adjacent to sch llhornite in chondrule *Ind-1* in ICM7 (Fig. 2); the chondrule (530

79 μm diameter) consists of clinoenstatite, interstitial albite, and sulfide patches (mainly troilite with
80 minor niningerite).

81 CHEMICAL COMPOSITION

82 Backscattered electron (BSE) images were obtained at Caltech using a ZEISS 1550VP field
83 emission SEM and a JEOL 8200 electron microprobe with solid-state BSE detectors. Four
84 quantitative WDS elemental microanalyses of type zolenskyite were carried out using the JEOL
85 8200 electron microprobe operated at 10 kV (for smaller interaction volume) and 8 nA in focused
86 beam mode. The focused electron beam is ~ 120 nm in diameter. The interaction volume for X-ray
87 generation in zolenskyite is ~ 800 nm in diameter, estimated using the Casino Monte Carlo
88 simulation of electron trajectory. Analyses were processed with the CITZAF correction procedure
89 (Armstrong 1995) using the Probe for EPMA program from Probe Software, Inc. Possible
90 interferences on peak position and background position were checked and corrected for all
91 measured elements based on WDS scans. Analytical results are given in Table 1. WDS scans did
92 not reveal other elements such as Na and Zn.

93 The empirical formula of type zolenskyite (based on 7 atoms *pfu*) is
94 $\text{Fe}_{0.99}\text{Mn}_{0.04}\text{Ca}_{0.01}\text{Cr}_{1.99}\text{S}_{3.98}$. The ideal formula is $\text{Fe}^{2+}\text{Cr}^{3+}_2\text{S}_4$, which is equivalent to a composition
95 of (in wt%): Fe 19.38, Cr 36.10, S 44.52.

96 Associated Cr-bearing troilite has an empirical formula (based on 4 atoms *pfu*) of
97 $(\text{Fe}_{0.97}\text{Cr}_{0.02})\text{S}_{1.00}$. Nearby clinoenstatite has an empirical formula (based on 6 atoms *pfu*) of
98 $(\text{Mg}_{1.95}\text{Fe}_{0.05})\text{Si}_2\text{O}_6$.

99

100

CRYSTALLOGRAPHY

101 Electron backscatter diffraction (EBSD) analyses, using methods described in Ma and
102 Rossman (2008, 2009), were performed using an HKL EBSD system on the ZEISS 1550VP Field-
103 Emission SEM, operated at 20 kV and 6 nA in focused-beam mode with a 70° tilted stage and in
104 a variable pressure mode (25 Pa). The focused electron beam is several nanometers in diameter.
105 The spatial resolution for diffracted backscattered electrons is ~30 nm in size. The EBSD system
106 was calibrated using a single-crystal silicon standard. The structure was determined and cell
107 constants were obtained by matching the experimental EBSD patterns with the known structures
108 of Fe-Cr-S and Cr-S phases, including FeCr₂S₄, (Fe_{0.6}Cr_{0.4})Cr₂S₄, and Cr₃S₄.

109 The EBSD patterns of all FeCr₂S₄ grains in the Indarch matrix are indexed only by the
110 *C2/m* CrNb₂Se₄-Cr₃S₄-type structure and give a best fit by the synthetic FeCr₂S₄ cell from Tressler
111 et al. (1968) (Fig. 3), in which $a = 12.84(1) \text{ \AA}$, $b = 3.44(1) \text{ \AA}$, $c = 5.94(1) \text{ \AA}$, $\beta = 117(1)^\circ$, $V =$
112 $234(6) \text{ \AA}^3$, and $Z = 2$. The mean angular deviation of the patterns is 0.38°. The calculated density
113 based on the empirical formula is 4.09 g/cm³. Calculated X-ray powder diffraction data for
114 zolenskyite are given in Table S1. The FeCr₂S₄ grain within chondrule *Ind-1* is daubr elite,
115 identified by EBSD to have a cubic spinel-type structure.

116 DISCUSSION

117 Zolenskyite (FeCr₂S₄) is the Fe-analog of brezinaite (Cr₃S₄), or the Cr-analog of heideite
118 (ideally FeTi₂S₄) (Keil and Brett 1974), joining the wilkmanite group. Zolenskyite is a monoclinic
119 polymorph of daubr elite.

120 It is unclear if some previous reports of daubr elite in enstatite chondrites are, in fact,
121 zolenskyite. Our analyses of zolenskyite in EH4 Indarch show it to be Zn free, thus differing from
122 the phase identified as daubr elite in EH3 Kota-Kota (5.2 wt.% Zn; Keil 1968) and EL3 MAC

123 88136 (up to 5.7 wt.% Zn; Lin et al. 1991). Grossman et al. (1985) reported FeCr_2S_4 in chondrules
124 in EH3 Qingzhen and identified the phase as daubr elite, but did not analyze it. Zincian daubr elite
125 is present in EH5 (4.3 wt.% Zn) and EL6 (up to 0.55 wt.% Zn) chondrites (Keil 1968) and
126 commonly occurs as exsolution lamellae in troilite parallel to $\{0001\}$ (e.g., Keil 1968; Rubin
127 1984). Daubr elite is also present as exsolution lamellae in troilite within the clastic matrix
128 component of EH3 Y-691 (Rubin et al. 2009).

129 Many aubrites (enstatite achondrites) contain small grains of daubr elite averaging 0.09
130 wt.% Zn (Watters and Prinz 1979). The Norton County aubrite breccia contains individual
131 daubr elite grains ranging up to 700 μm , associated with Ti-bearing troilite, ferroan and
132 ferromagnesian alabandite, and kamacite (Okada et al. 1988); daubr elite also occurs in Norton
133 County as exsolution lamellae in troilite.

134 It seems likely that the FeCr_2S_4 phase in enstatite chondrites and aubrites that occurs as
135 exsolution lamellae in troilite is daubr elite, but additional studies are required to determine which
136 FeCr_2S_4 polymorphs are present in different EH3 and EL3 chondrites. Any zolenskyite that may
137 have originally been present in unmetamorphosed enstatite chondrites could have transformed into
138 daubr elite in those samples that were heated to higher metamorphic temperatures (e.g., 800-
139 1000°C for EH5 and EH6 chondrites; Zhang et al., 1996).

140 Indarch EH4 consists principally of chondrules and moderately coarse interchondrule
141 material. It does not contain fine-grained matrix material (such as occurs in EH3 and EL3
142 chondrites; e.g., Rubin et al. 2009; Rubin 2010). A significant fraction of the interchondrule
143 material in Indarch is probably derived from crushed chondrules (e.g., Nelson and Rubin 2002).
144 In Indarch, the identification of daubr elite only in a chondrule and zolenskyite exclusively in the

145 matrix suggests that daubréelite formed at high temperatures during chondrule formation and that
146 zolenskyite formed from daubréelite in disaggregated chondrules by later-stage parent-body
147 processes.

148 Chondrules formed at high temperatures (in many cases ~1430-1730°C; e.g., Lofgren and
149 Lanier 1990; Radomsky and Hewins 1990) and very low pressures, consistent with the stability
150 field of daubréelite (Tressler et al. 1968). This can account for the presence of daubréelite in
151 Indarch chondrule *Ind-1*.

152 Experiments show that daubréelite can transform into zolenskyite at high pressures and
153 moderate temperatures (e.g., 5.5 GPa, 520°C; 3 GPa, 200°C) (Tessler et al. 1968). Such conditions
154 likely pertained in highly shocked EH6 chondrites (Rubin and Wasson 2011). Zolenskyite may
155 have formed from daubréelite in highly shocked regions of the EH parent asteroid, later to be
156 incorporated into Indarch as aberrant grains during small-scale impact-mixing events (e.g., Rubin
157 1990).

158 Whereas the daubréelite grain in the chondrule is optically homogeneous and unaltered
159 (Fig. 2), all zolenskyite grains in the matrix appear moderately altered (Fig. 1). This alteration
160 could be due to the same type of alkali metasomatic processes that occurred in EH3-chondrite
161 matrices and produced djerfisherite ($K_6(Fe,Cu,Ni)_{25}S_{26}Cl$) (El Goresy et al. 1988).

162 Indarch is apparently unbrecciated (Rubin, 2015) and only weakly shocked (shock-stage
163 S3; Rubin et al. 1997); its orthopyroxene grains exhibit undulose extinction and contain
164 clinoenstatite lamellae on (100). Because Indarch contains zolenskyite that likely formed at high
165 shock pressures, we suggest that annealing of the Indarch whole-rock to ~640°C (Huss and Lewis
166 1994) obliterated the evidence of brecciation.

167

168

IMPLICATIONS

169

170

171

172

173

174

175

ACKNOWLEDGMENTS

176

177

178

179

180

181

REFERENCES CITED

182

183

184

185

186

187

188

189

190

Indarch is a mildly metamorphosed EH4 chondrite. It contains the first-known natural occurrence of monoclinic FeCr₂S₄ (zolenskyite), a polymorph of daubréelite (cubic FeCr₂S₄). Zolenskyite probably formed from daubréelite at high shock pressures during collisions on the parent body. The phase may also occur in some other EH3 and EH4 chondrites; some previous reports of daubréelite in enstatite chondrites may actually be zolenskyite.

SEM, EBSD and EPMA were carried out at the Geological and Planetary Science Division Analytical Facility, Caltech, which is supported in part by NSF grants EAR-0318518 and DMR-0080065. This work was also supported by NASA grant NNG06GF95G (AER). We thank M. K. Weisberg, T. J. McCoy and Associate Editor S. B. Simon for their constructive reviews.

- Armstrong, J.T. (1995) CITZAF: A package of correction programs for the quantitative electron beam X-ray analysis of thick polished materials, thin films, and particles. *Microbeam Analysis*, 4, 177–200.
- El Goresy, A., Yabuki, H., Ehlers, K., Woolum, D., and Pernicka, E. (1988) Qingzhen and Yamato-691: A tentative alphabet for the EH chondrites. *Proceedings of the NIPR Symposium on Antarctic Meteorites*, 1, 65–101.
- Grossman, J.N., Rubin, A.E., Rambaldi, E.R., Rajan, R.S. and Wasson, J.T. (1985) Chondrules in the Qingzhen type-3 enstatite chondrite: Possible precursor components and comparison to ordinary chondrite chondrules. *Geochimica et Cosmochimica Acta*, 49, 1781–1795.

- 191 Huss, G.R. and Lewis, R.S. (1994) Noble gases in presolar diamonds II: Component abundances
192 reflect thermal processing. *Meteoritics*, 29, 811–829.
- 193 Isa, J., Ma, C., Rubin, A.E. (2016) Joegoldsteinite: A new sulfide mineral (MnCr_2S_4) from the
194 Social Circle IVA iron meteorite. *American Mineralogist*, 101, 1217–1221.
- 195 Keil, K. (1968) Mineralogical and chemical relationships among enstatite chondrites. *Journal of*
196 *Geophysical Research*, 73, 6945–6976.
- 197 Keil, K. and Brett, R. (1974) Heideite, $(\text{Fe,Cr})_{1+x}(\text{Ti,Fe})_2\text{S}_4$. a new mineral in the Bustee enstatite
198 achondrite. *American Mineralogist*, 59, 465–470.
- 199 Lin, Y.T., Nagel, H-J., Lundberg, L.L., and El Goresy, A. (1991) MAC88136 – The first EL3
200 chondrite (abstract). *Lunar Planet. Sci.*, 22, 811–812.
- 201 Lofgren, G.E. and Lanier, A.B. (1990) Dynamic crystallization study of barred olivine chondrules.
202 *Geochimica et Cosmochimica Acta*, 54, 3537–3551.
- 203 Lutz, H.D., Koch, U., and Siwert, H. (1983) Phase relationships of the ternary chromium sulfides
204 $\text{Cr}^{\text{II}}_{1-x}\text{M}_x\text{Cr}^{\text{III}}_2\text{S}_4$ (M = Mn, Fe, Co) with Cr_3S_4 and spinel structure. *Materials Research*
205 *Bulletin*, 18, 1383–1389.
- 206 Ma, C. (2021) Zolenskyite, IMA 2020-070, in: CNMNC Newsletter No. 59. *European Journal of*
207 *Mineralogy*, 33, DOI:10.5194/ejm-33-139-2021.
- 208 Ma, C. and Rossman, G.R. (2008) Barioperovskite, BaTiO_3 , a new mineral from the Benitoite
209 Mine, California. *American Mineralogist*, 93, 154–157.
- 210 Ma, C. and Rossman, G.R. (2009) Tistarite, Ti_2O_3 , a new refractory mineral from the Allende
211 meteorite. *American Mineralogist*, 94, 841–844.
- 212 Mason, B. (1966) The enstatite chondrites. *Geochimica et Cosmochimica Acta*, 30, 23–39.
- 213 Nelson, V.E. and Rubin, A.E. (2002) Size-frequency distributions of chondrules and chondrule
214 fragments in LL3 chondrites: Implications for parent-body fragmentation of chondrules.
215 *Meteoritics & Planetary Science*, 37, 1361–1376.
- 216 Okada, A., Keil, K., Taylor, G.J., and Newsom, H. (1988) Igneous history of the aubrite parent
217 asteroid: Evidence from the Norton County enstatite achondrite. *Meteoritics*, 23, 59–74.
- 218 Radomsky, P.M. and Hewins, R.H. (1990) Formation conditions of pyroxene-olivine and
219 magnesium olivine chondrules. *Geochimica et Cosmochimica Acta*, 54, 3475–3490.

- 220 Rubin, A.E. (1984) The Blithfield meteorite and the origin of sulfide-rich, metal-poor clasts and
221 inclusions in brecciated enstatite chondrites. *Earth and Planetary Science Letters*, 67,
222 273–283.
- 223 Rubin, A.E. (1990) Kamacite and olivine in ordinary chondrites: Intergroup and intragroup
224 relationships. *Geochimica et Cosmochimica Acta*, 54, 1217–1232.
- 225 Rubin, A.E. (2010) Physical properties of chondrules in different chondrite groups: Implications
226 for multiple melting events in dusty environments. *Geochimica et Cosmochimica Acta*, 74,
227 4807–4828.
- 228 Rubin, A.E. (2015) Impact features of enstatite-rich meteorites. *Chemie der Erde*, 75, 1–28.
- 229 Rubin A.E. and Wasson J.T. (2011) Shock effects in “EH6” enstatite chondrites and implications
230 for collisional heating of the EH and EL parent asteroids. *Geochimica et Cosmochimica*
231 *Acta*, 75, 3757–3780.
- 232 Rubin, A.E., Scott, E.R.D., and Keil, K. (1997) Shock metamorphism of enstatite chondrites.
233 *Geochimica et Cosmochimica Acta*, 61, 847–858.
- 234 Rubin, A.E., Griset, C.D., Choi, B.-G., and Wasson, J.T. (2009) Clastic matrix in EH3 chondrites.
235 *Meteoritics & Planetary Science*, 44, 589–601.
- 236 Tressler, R.E., Hummel, F.A., and Stubican, V.S. (1968) Pressure-temperature study of
237 sulfospinel. *Journal of the American Ceramic Society*, 51, 648–651.
- 238 Watters, T.R. and Prinz M. (1979) Aubrites: Their origin and relationship to enstatite chondrites.
239 *Proc. Lunar Planet. Sci. Conf.*, 10th, 1073–1093.
- 240 Zhang, Y., Huang, S., Schneider, D., Benoit, P.H., DeHart, J.M., Lofgren, G.E., and Sears, D.W.G.
241 (1996) Pyroxene structures, cathodoluminescence and the thermal history of the enstatite
242 chondrites. *Meteoritics & Planetary Science*, 31, 87–96.
- 243
- 244

245 **Table 1.** Average elemental composition of four point EPMA analyses for type zolenskyite.

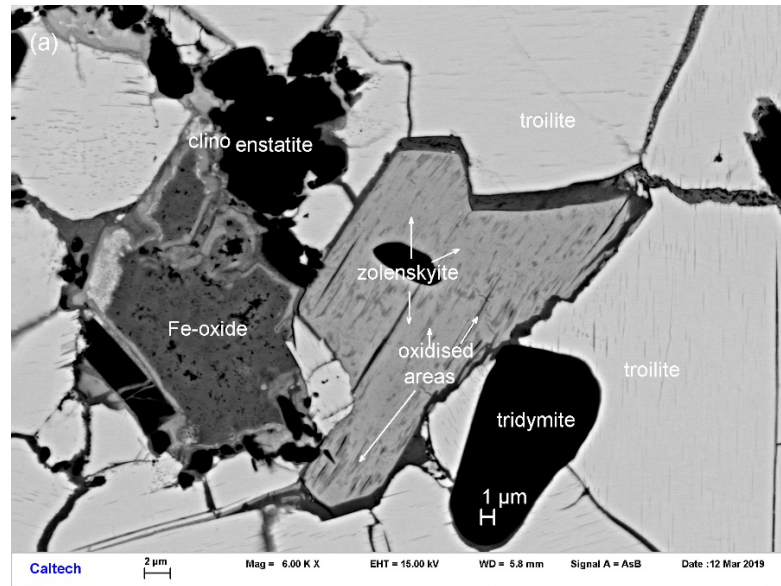
246

Constituent	wt%	Range	SD	Probe Standard
S	43.85	43.55-44.32	0.34	pyrite
Cr	35.53	34.18-36.76	1.24	Cr metal
Fe	18.94	17.72-20.36	1.22	pyrite
Mn	0.68	0.54-0.91	0.17	Mn metal
Ca	0.13	0.12-0.16	0.02	anorthite
Total	99.13			

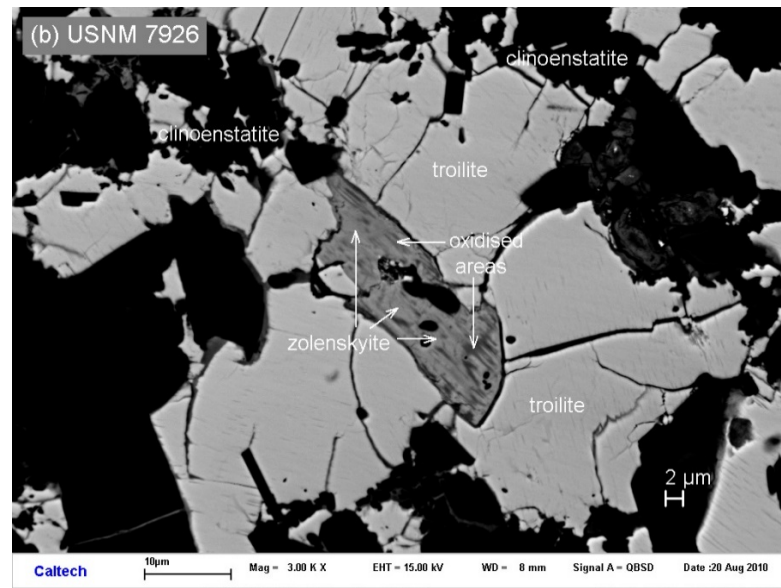
247

248

249
250



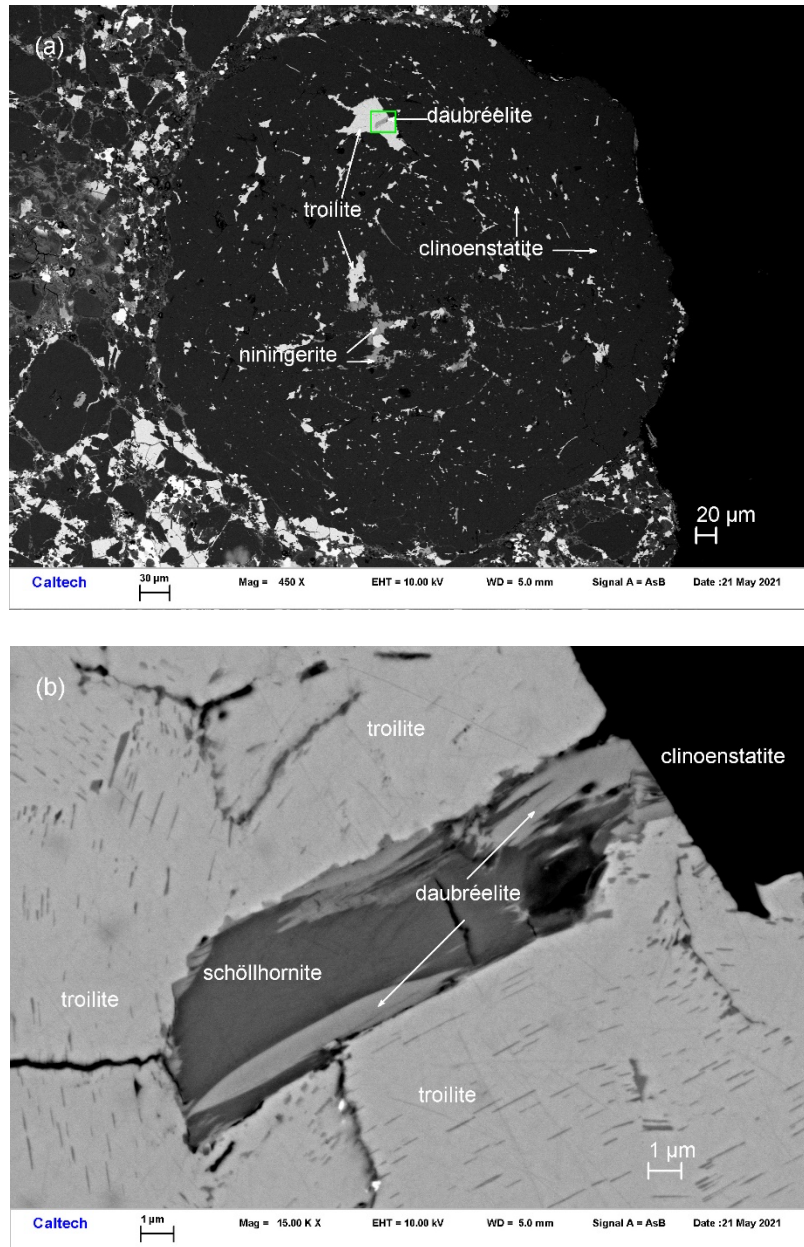
251
252



253
254

255 **Figure 1.** SEM BSE images showing zolenskyite with troilite, clinoenstatite, tridymite and Fe-
256 oxide in the Indarch matrix. (a) Section ICM1. (b) Section USNM 7926 (ICM3). In both cases,
257 the zolenskyite grains are flanked by a rind of oxidation/alteration products.
258

259
260
261



262
263

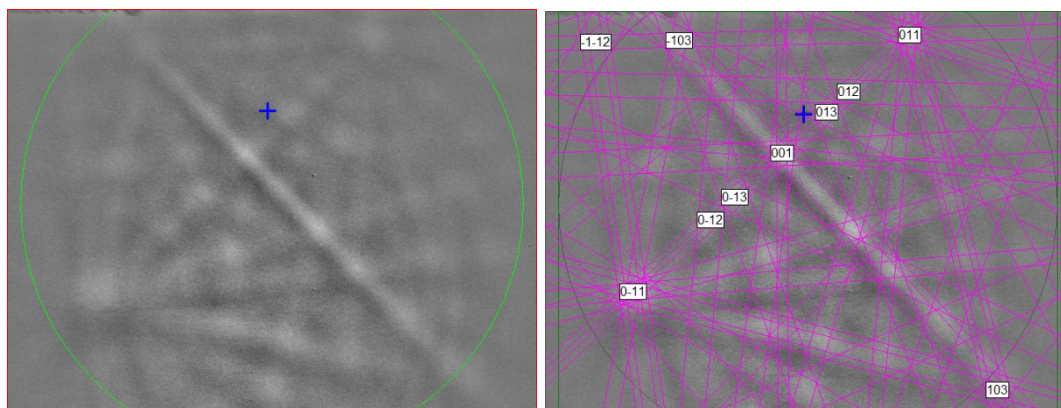
264
265

266 **Figure 2.** SEM BSE images of a porphyritic pyroxene chondrule *Ind-1* with sulfide-rich patches,
267 one of which contains daubrélite, in section ICM7. (a) Entire chondrule (530 μm diameter)
268 consists of clinoenstatite, interstitial albite, and sulfide patches. (b) High-magnification view
269 (small box in Fig. 2a) of an inclusion of daubrélite flanking schöllhornite within a patch of
270 troilite.

271

272

273
274



275
276
277
278
279

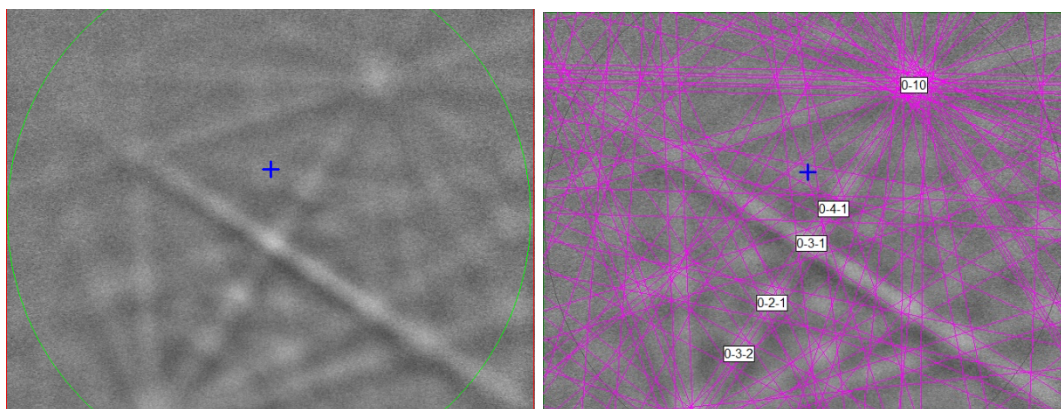


Figure 3. (left) EBSD patterns of the zolenskyite crystals in Figure 1 at different orientations, and (right) the patterns indexed with the $C2/m$ $FeCr_2S_4$ structure.